CHIN. PHYS. LETT. Vol. 38, No. 9 (2021) 092501

# Hyperon Dynamics in Heavy-Ion Collisions near Threshold Energy

Ding-Chang Zhang(张定昌), Hui-Gan Cheng(程辉淦), and Zhao-Qing Feng(冯兆庆)*

*School of Physics and Optoelectronic Technology, South China University of Technology, Guangzhou 510641, China*

(Received 30 April 2021; accepted 26 July 2021; published online 2 September 2021)

Within the framework of quantum molecular dynamics transport model, the isospin and in-medium effects on the hyperon production in the reaction of $^{197}\mathrm{Au}+{}^{197}\mathrm{Au}$ are investigated thoroughly. A repulsive hyperon-nucleon potential from the chiral effective field theory is implemented into the model, which is related to the hyperon momentum and baryon density. The correction on threshold energy of the elementary hyperon cross section is taken into account. It is found that the $\Sigma$ yields are suppressed in the domain of midrapidity and kinetic energy spectra with the potential. The hyperons are emitted in the reaction plane because of the strangeness exchange reaction and reabsorption process in the nuclear medium. The $\Sigma^-/\Sigma^+$ ratio depends on the stiffness of nuclear symmetry energy, in particular in the high-energy region (above 500 MeV).

DOI: 10.1088/0256-307X/38/9/092501

Heavy-ion collisions provide a good environment for studying the dense hadronic matter and in-medium properties of hadron, especially for strange particle production, which has attracted much attention. The hyperons may be created below the threshold energy in the heavy-ion collisions. The hyperon-nucleon (YN) interaction in theories[1–4] and YN scattering in experiments[5–7] have been studied, but the interaction of strange particles in dense nuclear matter and the dynamics of hyperon production in the high-density region are not well understood up to now. In pioneer works, the YN potential calculated by relativistic mean-field model (RMF) are generally attractive,[8–10] but a weak repulsive $\Sigma$N potential was argued.[11,12] Recently, the repulsive $\Sigma$N potential has been calculated by the Nijmegen extended-soft-core (ESC) potential model[13] and chiral effective field theory (EFT).[14] In particular, some relatively precise parameters of $\Sigma$N potential that is strongly isospin-dependent are obtained by EFT,[15] which will influence the strange particle dynamics in heavy-ion collisions.[16–18]

The equation of state in isospin asymmetric dense nuclear matter, namely the high-density symmetry energy, is not very clear up to now, which plays an important role in studying the properties and structures of neutron stars.[19] It is generally believed that hyperons will appear inside the neutron stars above $2\rho_0$.[20–22] The appearance of strange particles leads to the softening of the nuclear equation of state and less mass of neutron star.[23] The ingredients of hyperons in neutron stars are associated with the YN potentials. For instance, the attractive $\Sigma$N potential results in the appearance of $\Sigma$ in the low-density region in neutron stars before $\Lambda$. However, the repulsive $\Sigma$N potential leads to the disappearance of $\Sigma$.[24] The pressure gradient of the high-density nuclear matter generated via the heavy-ion collisions in high energy influences the hyperon emission in phase space. The collective flows of the ejected particles in heavy-ion collisions is related to the nuclear equation of state. It is a topical approach to extract the information of the high-density equation of state from the particle emission.[25]

The strangeness nuclear physics has been planned as one of topical issues by the large-scale scientific facilities in the world, for instance, the High Intensity heavy-ion Accelerator Facility (HIAF) in China,[26] the Alternating Gradient Synchrotron (AGS) at BNL in the United States,[27] the LHC-ALICE at the European Organization for Nuclear Research,[28] and the Japan Proton Accelerator Research Complex (J-PARC).[29] In theory, several models have been developed to describe the strange particle dynamics in heavy-ion collisions, such as the statistical model,[30] intranuclear cascade model,[31] and transport models.[32,33] The intensive investigation on the hyperon dynamics in heavy-ion collisions is helpful for extracting the high-density symmetry energy and YN interaction (potential, scattering, etc).

In this Letter, the in-medium properties of $\Sigma$ hyperons and nuclear symmetry energy in the domain of high-baryon densities are investigated with the Lanzhou quantum molecular dynamics (LQMD) transport model. The production of resonances with the mass below 2 GeV, hyperons ($\Lambda$, $\Sigma$, $\Xi$) and

Supported by the National Natural Science Foundation of China (Grant Nos. 12175072 and 11722546), and the Talent Program of South China University of Technology.

*Corresponding author. Email: fengzhq@scut.edu.cn

© 2021 Chinese Physical Society and IOP Publishing Ltd

mesons ($\pi$, $\eta$, $K$, $\overline{K}$, $\rho$, $\omega$) is coupled in the reaction channels via meson-baryon and baryon-baryon collisions.[34,35] The temporal evolutions of nucleons are described by Hamilton's equations of motion under the self-consistently generated two-body and three-body interaction potential with the Skyrme interaction. At the considered energies, the hyperons are mainly contributed from the channels of baryon–baryon and pion–baryon collisions. The symmetry energy in the LQMD model is composed of the kinetic energy from fermionic motion, the local interaction and the momentum potential at the saturation density with the value of 31.5 MeV.[36] The stiffness of symmetry energy is adjusted by the local part $E_{\rm sym}^{\rm loc} = \frac{1}{2}C_{\rm sym}(\rho/\rho_0)^{\gamma_{\rm s}}$ with $C_{\rm sym}$ being 38 MeV. The parameter $\gamma_{\rm s}$ is chosen to get the suitable case from constraining the isospin observables, e.g., the values of 0.5, 1 and 2 being the soft, linear and hard symmetry energy, respectively.

The evolution of hyperons is also determined by the Hamiltonian, which is given by

$$H_Y = \sum_{i=1}^{N_Y}\left[V_i^{\rm Coul} + V_{\rm opt}^{Y}(\boldsymbol{p}_i,\rho_i) + \sqrt{\boldsymbol{p}_i^2+m^2}\right], \quad (1)$$

where $N_Y$ is the total number of hyperons including charged resonances. Here $Y$ could be $\Lambda$, $\Sigma$ or $\Xi$ hyperons in our model. Here the Coulomb interaction $V_i^{\rm Coul}$ of hyperon and charged baryons takes the form of point charge. The $\lambda$ potential is calculated on the basis of the light-quark counting rule. The self-energies of hyperons are assumed to be two thirds of that experienced by nucleons, which leads to the $\Lambda$–nucleon potential in nuclear matter at the saturation density being the value of $-32$ MeV.[37] The $\Sigma$N optical potential is estimated by

$$\begin{aligned} V_{\rm opt}^{\Sigma}(\boldsymbol{p}_i,\rho_i) =& V_0(\rho_i/\rho_0)^{\gamma_{\rm s}} + V_1(\rho_n-\rho_p)t_\Sigma\rho_i^{\gamma_{\rm s}-1}/\rho_0^{\gamma_{\rm s}} \\ &+ C_{\rm mom}\rho_i\ln(\epsilon\boldsymbol{p}_i^2+1). \end{aligned} \quad (2)$$

Here, the isospin quantities are taken as $\boldsymbol{t}_\Sigma = 1$, 0, and $-1$ for $\Sigma^-$, $\Sigma^0$ and $\Sigma^+$, respectively. The $C_{\rm mom}$ and $\epsilon$ are 1.76 MeV and 500 $c^2$/GeV$^2$. The values of 14.8 MeV and 67.8 MeV for the isoscalar $V_0^\Sigma$ and isovector $V_1^\Sigma$ parts are taken by fitting the results from the next-to-leading order (NLO) in chiral EFT with a cutoff of 600 MeV.[15] The hyperon dynamics in heavy-ion collisions is influenced by the optical potential. The energy conservation is satisfied with the threshold energy correction and invariant energy during the hyperon production. Shown in Fig. 1 is the $\Sigma$ optical potential as functions of density and momentum. The difference of the potentials with the isospin splitting is obvious with the baryon density. The effective mass $m_Y^* = V_{\rm opt}^Y(p=0,\rho_i) + m_Y$ is implemented into the threshold energy correction for the hyperon creation. It is obvious that the repulsive potential will enhance the threshold energy and consequently results in the reduction of hyperon production. In contrast, the attractive potential manifests an opposite contribution.

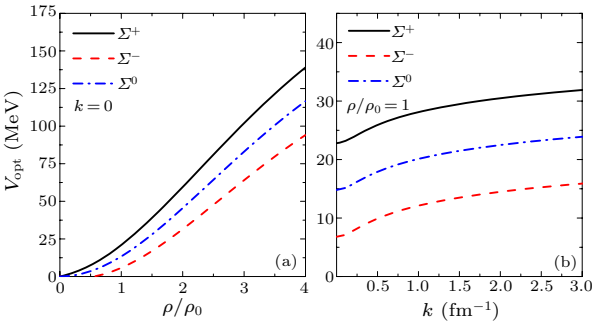


**Fig. 1.** (a) The density and (b) momentum dependence of hyperon-nucleon optical potential.

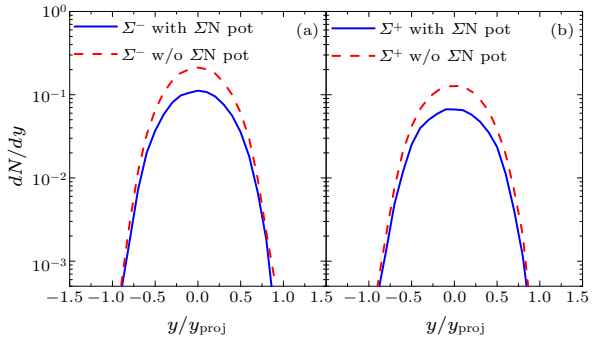


**Fig. 2.** The rapidity distribution of (a) $\Sigma^-$ and (b) $\Sigma^+$ in the central $^{197}$Au + $^{197}$Au collisions at an incident energy of 2 A GeV.

The heavy-ion collisions provide a unique environment for creating the high temperature and dense hadronic matter in laboratories. The strange particles are produced during the compressed stage in two colliding nuclei. The evolutions are deviated by the surrounding baryons via the interaction potential and rescattering process. The dynamics of strange particles is associated with the high-density equation of state, i.e., the rapidity distribution, energy spectra, collective flow etc. Shown in Fig. 2 is the rapidity distribution of $\Sigma$ hyperon in the $^{197}$Au + $^{197}$Au collisions at an incident energy of 2 A GeV. It is obvious that the hyperons are produced mainly in the central rapidity region. At the considered energies, hyperons are mainly created via the nucleon–nucleon and pion–nucleon collisions as the channels $NN \to NYK$ and $N\pi \to YK$. The $\Sigma^+$ and $\Sigma^-$ as the charged hyperon are affected by the Coulomb interaction and optical potential in the nuclear medium. The influence of the optical potential on charged $\Sigma^\pm$ is obvious. The hyperons are favorable to escape from the reaction zone instead of being captured by surrounding nucleons with the repulsive potential. The isospin-dependent

$\Sigma$N potential influences the threshold energy. Consequently, the lower threshold energy of $\Sigma^-$ enhances the yields in nucleon–nucleon collisions. The influence of YN potential and the stiffness of symmetry energy on the final multiplicities of hyperons is listed in Table 1. The hyperon yields are obviously reduced with the YN potential. The $\Sigma^-/\Sigma^+$ ratio is nearly independent of the potential but weakly modified by the symmetry energy.

**Table 1.** The final multiplicity of hyperons and the isospin ratio $\Sigma^-/\Sigma^+$ in the central $^{197}$Au + $^{197}$Au collisions with different symmetry energies and YN potentials.

| Beam energy | Stiffness of symmetry energy | $\Lambda$ | $\Sigma^-$ | $\Sigma^+$ | $\Sigma^0$ | $\Sigma^-/\Sigma^+$ |
|---|---|---|---|---|---|---|
| 1.5 A GeV | Soft (with $\Sigma$N pot.) | 0.1008 | 0.0249 | 0.0143 | 0.0168 | 1.736 |
| 1.5 A GeV | Hard (with $\Sigma$N pot.) | 0.1002 | 0.0247 | 0.0141 | 0.0167 | 1.754 |
| 2 A GeV | Soft (with $\Sigma$N pot.) | 0.3813 | 0.1015 | 0.0627 | 0.0727 | 1.616 |
| 2 A GeV | Hard (with $\Sigma$N pot.) | 0.3777 | 0.1011 | 0.0619 | 0.0726 | 1.632 |
| Beam energy | YN potential | $\Lambda$ | $\Sigma^-$ | $\Sigma^+$ | $\Sigma^0$ | $\Sigma^-/\Sigma^+$ |
| 2 A GeV | Without potential | 0.6294 | 0.1694 | 0.1052 | 0.1232 | 1.610 |
| 2 A GeV | With potential | 0.3652 | 0.0918 | 0.0571 | 0.0683 | 1.607 |

The YN potential will influence the phase-space distribution of hyperons produced in the heavy-ion collisions. The kinetic energy spectra of particle emission can be used to extract the in-medium properties of hadrons and the stiffness of symmetry energy. Shown in Fig. 3 is a comparison of the kinetic energy spectra of $\Sigma^-$ and $\Sigma^+$ with the different case of $\Sigma$N potential and the isospin ratio $\Sigma^-/\Sigma^+$. It is obvious that the hyperon production is reduced with the potential and the difference of charged hyperons is pronounced. The evolution of charged $\Sigma$ hyperon is influenced by the Coulomb interaction and the optical potential. The elementary cross section for hyperon production is modified via the threshold energy. The reduction of hyperon yields is caused by the enhancement of threshold energy. The in-medium effect exists in the whole energy spectra. Hyperons in the high-energy region are more likely to be ejected from the fire ball formed in heavy-ion collisions and can be probes for investigating the properties of dense baryonic matter. The hunting of sensitive observables for probing the high-density symmetry energy in heavy-ion collisions or from the merging of binary neutron stars attracted much attention. Particles emitted during the compression stage in heavy-ion collisions are promising observables. In earlier studies, Li applied the pion production in heavy-ion collisions for extracting the equation of state of asymmetric nuclear matter, and proposed the $\pi^-/\pi^+$ ratio for extracting the high-density behavior of symmetry energy.[38] Moreover, the feasibility of studying high-density symmetry energy by $\Sigma^-/\Sigma^+$ ratios was also investigated by the UrQMD transport model.[39] Different from the pions, which may be produced in the low and high density region, amount of $\Sigma$ hyperons are mainly created in the high-density domain in the nucleus–nucleus collisions. It may be a better observable for probing the high-density symmetry energy. The kinetic energy spectra of the isospin ratio $\Sigma^-/\Sigma^+$ with different symmetry energies is shown in the lower panels. The solid and dashed lines are fitting from the calculations for guiding eyes. It is roughly 5% difference between the hard and soft symmetry energies at kinetic energies above 700 MeV, which is caused by both the threshold energy correction and transportation of hyperons and nucleons. The $\Sigma^-/\Sigma^+$ ratio could be a good probe for extracting the behavior of high-density symmetry energy. Further experiments are expected at the HIAF facility in the near future.

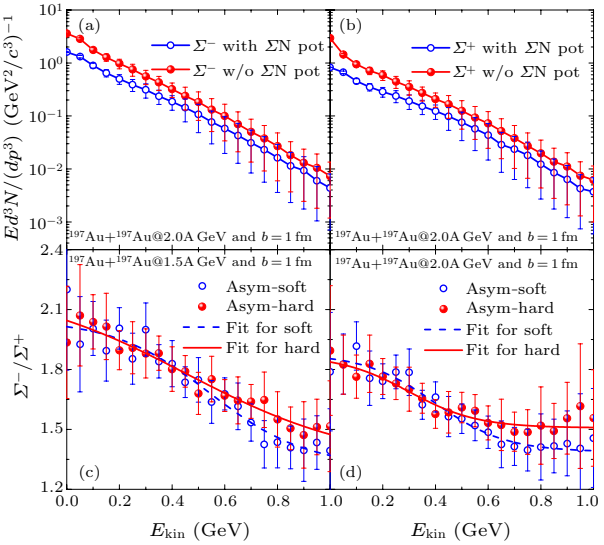


**Fig. 3.** The kinetic spectra of (a) $\Sigma^-$ and (b) $\Sigma^+$ in the reaction of $^{197}$Au + $^{197}$Au at 2 A GeV with the $\Sigma$N potential and the isospin ratio $\Sigma^-/\Sigma^+$ with the different stiffness of symmetry energy in the reaction of $^{197}$Au + $^{197}$Au at (c) 1.5 A GeV and (d) 2 A GeV, respectively. The lines are shown for guiding the eyes.

The schematic diagram of directed flow and elliptic flow are given in Fig. 4. The directed flow shows the degree of deflection of the particles' momentum direction from the beam direction, which comes from the pressure gradient of nuclear matter formed in heavy-ion collisions. The larger the compressed nuclear mat-

ter pressure, the greater the degree of deflection of the particles' momentum direction. Therefore, the directed flow is a sensitive physical quantity that is directly dependent on the nuclear equation of state. The elliptic flow gives the difference between in-plane and out of plane emission of hyperons, and reflects the ability to transform the position space inhomogeneity to momentum space inhomogeneity in heavy-ion collision. The flow information can be expressed as the first and second coefficients from the Fourier expansion of the azimuthal distribution as $\frac{dN}{d\phi}(y, p_t) = N_0 [1 + 2v_1(y, p_t)\cos(\phi) + 2v_2(y, p_t)\cos(2\phi)]$, where $p_t = \sqrt{p_x^2 + p_y^2}$ and $y$ are the transverse momentum and the longitudinal rapidity along the beam direction, respectively. The elliptic flow $v_2 = \langle (p_x^2 - p_y^2)/p_t^2 \rangle$ manifests the competition between the in-plane ($v_2 > 0$) and out-of-plane ($v_2 < 0$, squeeze-out) particle emissions. Calculations are performed in the semi-central collisions with the impact parameters of $b = 4$ fm. The E895 data for the $\Lambda$ in-plane flow at AGS energies[40] are well reproduced with the model. The collective flows of $\Sigma$ hyperons are similar to the structure of $\Lambda$, which manifests the well-known S shape for the transverse flow and the small $v_2$ values. The YN potential and Coulomb interaction affect the hyperon emission in phase space. The precise measurements on the hyperon flows are helpful for investigating the YN, YY potential and high-density symmetry energy.

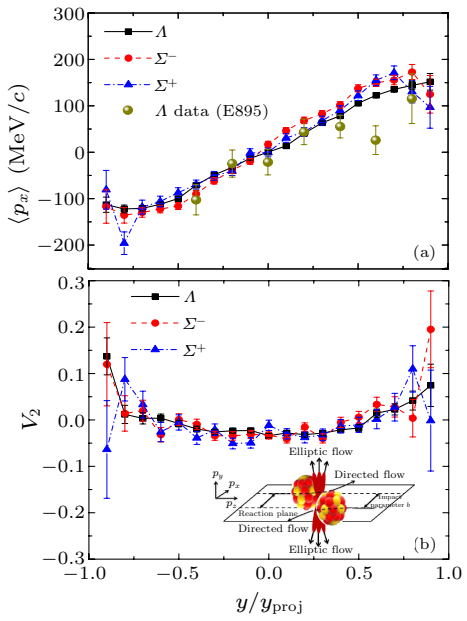


**Fig. 4.** (a) The transverse and (b) elliptic flows of $\Lambda$, $\Sigma^-$ and $\Sigma^+$ in the $^{197}$Au + $^{197}$Au collisions at 2 A GeV. The experimental data of $\Lambda$ production from E895 Collaboration[40] are shown for comparison.

In summary, the hyperon dynamics and the collective flows in the $^{197}$Au + $^{197}$Au collisions at 2 A GeV have been investigated within the LQMD model. The rapidity distribution and kinetic energy spectra of $\Sigma$ hyperons are calculated. It can be seen that the rapidity distribution and kinetic energy distribution of $\Sigma$ hyperons are sensitive to the hyperon-nucleon potential. The hyperons are produced mainly in the central rapidity region in heavy-ion collisions. The repulsive optical potential increases the threshold energy of hyperons, which results in the decrease of the number of hyperons in the middle rapidity region and in the low kinetic energy. The $\Sigma^-/\Sigma^+$ energy spectra are dependent on the stiffness of symmetry energy. The ratio of $\Sigma^-/\Sigma^+$ could be a sensitive observable to extract the information of symmetry energy in nuclear matter, especially the high density part. More experiments on the hyperon production in heavy-ion collisions are expected at the HIAF in the near future. Moreover, the collective flows of hyperons are analyzed and, the transverse flow especially, compared with the experimental data from the E895 Collaboration. It is found that the emission of hyperons in the high rapidity region is increased slightly by the repulsive potential.

## References


[1] Haidenbauer J and Meißner U G 2005 *Phys. Rev. C* **72** 044005
[2] Dai L R, Zhang Z Y, Yu Y W and Wang P 2003 *Nucl. Phys. A* **727** 321
[3] Fujiwara Y, Nakamoto C, Suzuki Y *et al.* 2004 *Prog. Theor. Phys. Suppl.* **156** 17
[4] Fujiwara Y, Suzuki Y and Nakamoto C 2007 *Prog. Part. Nucl. Phys.* **58** 439
[5] Nagata J, Yoshino H, Limkaisang V *et al.* 2002 *Phys. Rev. C* **66** 061001(R)
[6] Kadowaki T, Asai J, Imoto W *et al.* 2002 *Eur. Phys. J. A* **15** 295
[7] Kondo Y, Ahn J K, Akikawa H *et al.* 2000 *Nucl. Phys. A* **676** 371
[8] Rufa M, Schaffner J, Maruhn J *et al.* 1990 *Phys. Rev. C* **42** 2469
[9] Lombard R J Marcos S and Mareš J 1995 *Phys. Rev. C* **51** 1784
[10] Batty C J 1979 *Phys. Lett. B* **87** 324
[11] Gal A, Hungerford E V and Millener D J 2016 *Rev. Mod. Phys.* **88** 035004
[12] Dover C B, Millener D J and Gal A 1989 *Phys. Rep.* **184** 1
[13] Rijken T A, Nagels M M and Yamamoto Y 2010 *Nucl. Phys. A* **835** 160
[14] Petschauer S, Haidenbauer J, Kaiser N *et al.* 2016 *Eur. Phys. J. A* **52** 15
[15] Haidenbauer J and Meißner U G 2015 *Nucl. Phys. A* **936** 29
[16] Ga J H, Ma G L, Pu S *et al.* 2020 *Nucl. Sci. Tech.* **31** 90
[17] Lv H, Zhang S S, Zhang Z H *et al.* 2018 *Chin. Phys. Lett.* **35** 062102
[18] He Y J, Gu C C, Su J *et al.* 2020 *Nucl. Sci. Tech.* **31** 84
[19] Xu Y, Zhi Q J, Wang Y B *et al.* 2019 *Chin. Phys. Lett.* **36** 061301
[20] Weber F 2005 *Prog. Part. Nucl. Phys.* **54** 193
[21] Jiang W Z, Li B A, Chen L W 2012 *Astrophys. J.* **756** 56
[22] Tsuruta S, Sadino J, Kobelski A *et al.* 2009 *Astrophys. J.* **691** 621
[23] Baldo M, Birgio G F, Schulze H J 2000 *Phys. Rev. C* **61**

055801
[24] Schaffner-Bielich J, Hanauske M, Stöcker H and Greiner W 2002 *Phys. Rev. Lett.* **89** 171101
[25] Yan T Z, Li S, Wang Y N *et al.* 2019 *Nucl. Sci. Tech.* **30** 15
[26] Yang J C, Xia J W, Xiao G Q *et al.* 2013 *Nucl. Instrum. Methods B* **317** 263
[27] Pinkenburg C, Ajitanand N N, Alexander J M *et al.* 1999 *Phys. Rev. Lett.* **2743** 68
[28] Dönigus B 2013 *Nucl. Phys. A* **904–905** 547c
[29] Tamura H 2012 *Prog. Theor. Exp. Phys.* **2012** 02B012
[30] Andronic A, Braun-Munzinger P, Stachel J *et al.* 2011 *Phys. Lett. B* **697** 203
[31] Cugnon J, Deneye P and Vandermeulen J 1989 *Nucl. Phys. A* **500** 701
[32] Hartnack C, Oeschler H, Leifels Y, Bratkovskaya E and Aichelin J 2012 *Phys. Rep.* **510** 119
[33] Buss O *et al.* 2012 *Phys. Rep.* **512** 1
[34] Feng Z Q 2011 *Phys. Rev. C* **84** 024610
[35] Feng Z Q 2018 *Nucl. Sci. Tech.* **29** 40
[36] Feng Z Q 2012 *Phys. Rev. C* **85** 014604
[37] Feng Z Q 2013 *Nucl. Phys. A* **919** 32
[38] Li B A 2002 *Phys. Rev. Lett.* **88** 192701
[39] Li Q F, Li Z X, Zhao E G *et al.* 2005 *Phys. Rev. C* **71** 054907
[40] Chung P, Ajitanand N N, Alexander J M *et al.* 2001 *Phys. Rev. Lett.* **86** 2533